

# Dynamic Security Constrained Optimal Power Flow Using Finite Difference Sensitivities

Shrirang Abhyankar *Member, IEEE*, Vishwas Rao, Mihai Anitescu

**Abstract**—We present a novel technique for determining the solution of optimal power flow, including dynamic security constraints, using forward sensitivities computed by using finite differences. Finite differencing provides an easy way of computing the sensitivities of the dynamic security constraints in optimal power flow. A dynamic security measure based on the frequency excursion of the generators is presented. Our formulation also yields the marginal cost associated with the generator’s frequency excursion.

**Index Terms**—Optimal power flow, Dynamic security, Transient stability, Frequency deviation, Finite differencing, Marginal cost of frequency deviation.

## I. INTRODUCTION

Optimal power flow (OPF) is a widely used and important tool in power system analysis. The solution of the optimal power flow ensures an economic power system operation while satisfying the operational security constraints. However, such a solution is valid only for steady-state operation. An optimal power flow solution does not guarantee that the power system will be dynamically secure when subjected to credible contingencies such as short-circuit faults or loss of generators, transmission lines, or loads. Dynamic security is a concern for system planning and operations experts because of significant higher penetrations of renewable energy resources, most of which are electronically coupled to the grid, are expected in the future. This situation presents new technical challenges, particularly in the reduction of system inertia through the displacement of conventional generation resources during light load periods [1]. Thus, ensuring dynamic security, along with the optimal and secure steady-state operation is an important emerging problem.

## II. LITERATURE REVIEW

One of the first approaches for solving transient stability constraints in an optimal power flow was proposed in [2]; a transient energy function was used to model the dynamic constraints in an optimal power flow. Incorporation of dynamic security constraints as equality constraints in the form of discretized differential equations and inequality constraints for bounds on the trajectory was introduced in [3]. The dynamic security constraints were incorporated through a potential energy boundary surface formulation with the transient stability discretized differential-algebraic equations as the equality

constraints. Gan et al. [4] used a similar discretize-then-optimize approach and used the deviation of rotor angles as the transient stability constraint. A dynamic security preventive control also has been proposed using pattern recognition techniques [5], [6] and artificial neural networks [7], [8]. An evaluation of the maximum allowable transfer enforcing transient stability constraints was presented in [9]; specifically, a single machine equivalent (SIME) approach was used to identify the critical contingencies and shift the generation from the critical machines to the non critical ones.

Chen et al. [10] presented constraint transcription technique. In their approach, a single inequality constraint for the dynamics is computed through an averaging of the inequality constraint at each time step. Thus a significant reduction in the dimensionality of the problem is achieved as compared with the discretize-then-optimize approach. A solution of the optimal power flow with multi-contingency transient stability constraints was presented in [11]. A forward trajectory sensitivity approach was also used in [12] to obtain a suboptimal solution of the dynamic security-constrained OPF problem. An adjoint method for computing the sensitivities for the constraint transcription technique was used in [13]. Evolutionary algorithms using particle swarm optimization, genetic algorithms, and neural networks were presented in [14]–[21]

In this work, we present a finite difference computed sensitivity-based approach to the dynamic security constrained OPF problem. Sensitivity-based approaches have the advantage of much smaller memory footprint which may be a concern in real-time oriented architectures that are leading target architectures for the deployment of such optimization strategies. Here, the trajectory sensitivities are used for calculating the generation that needs to be shifted from the most advanced generators, in terms of the generator speed deviation, to the least advanced. A particular challenge are the path constraints on the system dynamics that need to be expressed in parameter space (OPF state space) to take full advantage of the benefits of sensitivity approaches. They would typically result in nonsmooth approaches; we present a penalty approach to allow for a smooth treatment that is compatible with Newton-type methods.

## III. DYNAMIC SECURITY CONSTRAINED OPTIMAL POWER FLOW

The dynamic security-constrained optimal power flow (DSOPF) formulation combines the OPF equations with the transient stability equations as given in (1)–(6). In addition, the dynamics trajectory must satisfy security constraints at each

Shrirang Abhyankar (e-mail: abhyshr@mcs.anl.gov) and Mihai Anitescu (e-mail: anitescu@mcs.anl.gov) are with the Mathematics and Computer Science Division, Argonne National Laboratory, Argonne, IL 60439.

Vishwas Rao (e-mail: visrao@vt.edu) is with the Department of Computer Science, Virginia Tech, Blacksburg, VA, 24060.

time step as given by (7).

$$\min \quad C(p) \quad (1)$$

$$\text{s.t.} \quad g_s(p) = 0 \quad (2)$$

$$h_s(p) \leq h^+ \quad (3)$$

$$p^- \leq p \leq p^+ \quad (4)$$

$$\dot{x} = f(x, y, p, \lambda), \quad x(t_0) = I_{x0}(p) \quad (5)$$

$$0 = g(x, y, p, \lambda), \quad y(t_0) = I_{y0}(p) \quad (6)$$

$$h(x(t), y(t)) \leq 0, \quad \forall(t) \quad (7)$$

Here,  $p \equiv [P_g, Q_g, \theta, V]^T \in \mathbb{R}^{np}$  are the OPF variables, namely the real and reactive power generation and the bus voltage magnitudes and angles. The steady-state security constraints are given by (2)-(4).

Equations (5) and (6) describe the differential-algebraic-discrete (DAD) model of the power system [12].  $I_{x0}$  and  $I_{y0}$  are functions that describe the relation between the initial conditions,  $(x(t_0), y(t_0))$ , for the DAD and the optimization variables  $p$ . Here,  $x \in \mathbb{R}^{nx}$  represents the dynamic states for the machines and its associated controllers;  $y \in \mathbb{R}^{ny}$  represents the algebraic states, namely, the network bus voltages; and  $\lambda$  denotes the action of discrete events such as fault incidence/removal, transmission line switching, load loss, or generation tripping. Equation (7) gives a measure of the dynamic security of the system at each time step. An example of (7) is the separation of generator rotor angles that has been extensively as a dynamic security criterion in the literature [4], [11], [22].

We note here that, seen in the full parameter-state space, the DSOPF problem is an infinite-dimensional problem with infinite dynamic constraints. However, given that  $x, y$  at any given time  $t$  can be computed from the initial conditions  $x(t_0), y(t_0)$  and the initial conditions are functions of the OPF variables,  $x, y$  are implicit functions of  $p$ . Thus, the original DSOPF problem can be expressed only in terms of the optimization variables as given in (8).

$$\min \quad C(p)$$

$$\text{s.t.} \quad g_s(p) = 0$$

$$h_s(p) \leq h^+ \quad (8)$$

$$p^- \leq p \leq p^+$$

$$h(x(p, t), y(p, t)) \leq \rho, \quad \forall(t)$$

Due to the infinite number of constraints and finite number of parameters, this is a semi-infinite optimization problem [23], and can in principle be solved as such if one adopts a direct transcription approach [24]. To allow for sensitivity approaches, we consider aggregating the path constraints, as can be achieved by using the minmax form  $\max_t \{0, h_i(x(p, t), y(p, t))\} = 0$ , where  $h_i$  is a component of  $h$ . This however, leads to nonsmooth optimization problems that are considerably harder to solve practically than their smooth counterparts [25].

To allow for smooth approaches, we use a constraint aggregating procedure, based on smoothing the minmax constraint.

[26]. Instead of enforcing the constraints at each time step, the evolution of the constraint surface at some final time can be used as a constraint [10].

$$H(x(p, t), y(p, t)) = \sigma \int_0^T [\max(0, h(x(p, t), y(p, t)))]^\eta dt = 0 \quad (9)$$

Here,  $\eta$  is an exponent to ensure sufficient smoothness of (9), and  $\sigma$  is a multiplier, similar to penalty cost term, to ensure a decent progress of the optimization. Its value should be large enough to ensure smoothness, but not too large to promote degeneracy; a value around  $\eta = 2$  would be appropriate to this end. Since the equality constraint in (9) cannot be easily handled by optimization solvers [10], an inequality constraint  $H(x, y) \leq \rho$  is used instead, where  $\rho$  is a positive small number.

With this formulation, replacing the path constraints by  $H(x, y) \equiv H(p)$  with  $H$  defined by (9) in (8) completely defines a smooth problem of  $p$  only that we can solve with smooth optimization tools.

#### IV. MEASURE OF DYNAMIC SECURITY

We use frequency deviation of the generators as a measure of dynamic security in our analysis. Frequency regulation is an important issue in dynamic security and the synchronous generators are operated within stringent regulations around the nominal operating frequency [27]. Significant deviation above nominal frequency can cause tripping of generating units, while under frequency can cause shedding of loads or operation of protective devices. Accordingly, we model the dynamic security constraint as given by (10).

$$H_i(x, y) = \sigma \int_0^T [\max(0, \omega_i - \omega^+, \omega^- - \omega_i)]^\eta dt \quad (10)$$

$$i = 1, \dots, m$$

Here  $\omega_i$  is the synchronous speed of the generator  $i$  that governs its frequency, and  $m$  equals the number of generators. Thus, our formulation uses  $H(x, y) \in \mathbb{R}^m$  dynamic constraints appended to the OPF instead of a single inequality constraint as used in [10]. Having separate constraints provides a finer violation measure in terms of the frequency excursion for each generator, and its Lagrange multiplier gives the associated marginal cost.

#### V. COMPUTING DERIVATIVES VIA FINITE DIFFERENCING

Equation (8) can be solved by any standard nonlinear optimization solver such as an interior point method or reduced-set method. However, the optimization solver requires the derivative of  $H(x(p), y(p))$  with respect to optimization variables  $p$ , which is a non trivial computing task. For a rigorous derivation of the gradient of  $H(x(p), y(p))$ , see [10], [28].

$$\nabla_p H(x, y) = \sigma \int_0^T \frac{\partial [\max(0, h(x(t), y(t)))]^\eta}{\partial p} dt \quad (11)$$

In this work, we tackle the calculation of (11) by using finite differencing. Derivative calculation with finite differencing is an easy, yet powerful, approach used in various fields where

the derivative is unavailable or difficult to obtain. It is based on Taylor series truncated at various orders of expansion. A sequence of finite difference approximations gives the gradient. Consider the cost function  $H_i(x(p), y(p))$ , where  $p \in \mathbb{R}^{np}$ . The cost function is defined from  $\mathbb{R}^{np} \rightarrow \mathbb{R}$ . Now the partial derivative with respect to the  $k^{\text{th}}$  component of  $p_*$  can be approximated as follows

$$\frac{\partial H_i}{\partial p_k}(p_*) \approx \frac{H_i(x(p_* + \epsilon e_k), y(p_* + \epsilon e_k)) - H_i(x(p_*), y(p_*))}{\epsilon} \quad (12)$$

Here  $e_k$  is the  $k^{\text{th}}$  canonical basis vector and  $\epsilon$  is a small perturbation. The gradient with respect to  $p$  performing the computation is shown in Equation (12) for  $k = 1, 2, \dots, np$ . The gradient can be written as

$$\nabla_p H_i(x(p), y(p)) = \begin{bmatrix} \frac{\partial H_i}{\partial p_1}(p_*) & \frac{\partial H_i}{\partial p_2}(p_*) & \dots & \frac{\partial H_i}{\partial p_{np}}(p_*) \end{bmatrix}^T \quad (13)$$

The approximation in Equation (12) is first-order accurate. The accuracy can be improved by performing central finite differencing. However, this requires an extra cost function evaluation for each evaluation of the partial derivative. The approximations by central finite differencing are second-order accurate and can be written as

$$\frac{\partial H_i}{\partial p_k}(p_*) \approx \frac{H_i(x(p_* + \epsilon e_k), y(p_* + \epsilon e_k)) - H_i(x(p_* - \epsilon e_k), y(p_* - \epsilon e_k))}{2\epsilon} \quad (14)$$

It is important to choose the right  $\epsilon$  to get good approximations. One of the factors to consider is the ratio of  $\epsilon$  and  $p_k$ . A guideline for its selection is that it should be greater than but close to the square root of the round-off error.

## VI. TEST CASE AND SIMULATION RESULTS

The test case, shown in Fig. 1, used in this work is the 3-generator, 9-bus system available in [29] Chapter 7. All generators use a 4<sup>th</sup> order two-axis model with an IEEE Type-1 exciter. The objective function (1) used in this work is the minimization of the total generation cost where the cost for each generator's real power output is given by a second order polynomial term  $C(p) = \sum_{i=1}^m (\alpha P_{gi}^2 + \beta P_{gi} + \gamma)$ . The cost coefficients used are from the MATPOWER [30] package.

The proposed scheme is implemented in MATLAB by using its nonlinear optimization solver *fmincon* available through its optimization toolbox. An interior-point method, available in *fmincon*, is used to solve the the TSOPF problem. To avoid the complication of computing the Hessian analytically or the additional error that would stem from finite difference approximations (which are less accurate for Hessian than they are for gradients), we use a quasi-Newton BFGS scheme, available with *fmincon*, to approximate the Hessian.

For the numerical discretization of the DAE equations, an implicit-trapezoidal (Crank-Nicholson) scheme is employed

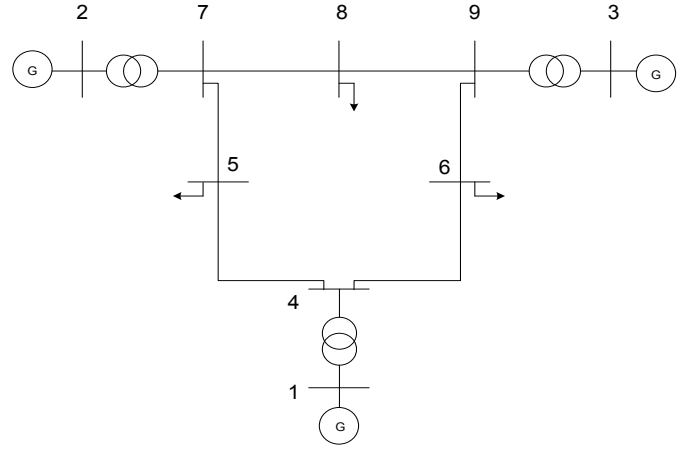


Fig. 1. 3-generator, 9-bus test case system

with a time-step of 0.01667 seconds. We used coefficients  $\sigma=5e3$  and  $\eta=2$  for computing the dynamics constraint function given by (10). We note that the choice of  $\sigma$  is heuristic and dependent on the system conditions. A forward differencing approach is used for computing  $\nabla_p H(x(p), y(p))$  using a perturbation of  $\epsilon=1e-5$ . We note that the gradient calculation using forward finite differencing entails  $np$  runs, one for each component of  $p$ , of the DAE solver. While this may be seem onerous, especially for large systems, it is perfectly parallelizable since it is an embarrassingly parallel calculation. We have not done this derivative calculation in parallel in our current implementation, but it is a part of our future work.

### A. OPF without dynamic security constraints

The generation schedule obtained from OPF without dynamic security constraints is presented in Table I. The total cost for this schedule is \$5921.47/hr. We note here that Gen2 has the maximum power dispatch since it is the cheapest generator.

TABLE I  
GENERATION SCHEDULE WITHOUT DYNAMIC CONSTRAINTS

Generator	Bus Number	MW
Gen1	1	89.81
Gen2	2	134.33
Gen3	3	94.20

To assess the dynamic security of this OPF solution, we considered two cases for a self-clearing 3-phase solid fault on Bus 7 and Bus 9. The fault lasts for 12 cycles, initiating at  $t=0.1$  seconds and extinguishing at  $t=0.3$  seconds. The system is considered to be dynamically secure if the frequency of the generators does not exceed the upper and lower frequency limits of 60.8 Hz and 59.2 Hz, respectively, that is, a deviation of 0.8 Hz from the nominal frequency. The dynamic security measure given by Equation 10 with these limits is shown in Figure 2. As seen in Figure 3, for the fault at Bus 7, the system is not dynamically secure, since the generator frequencies

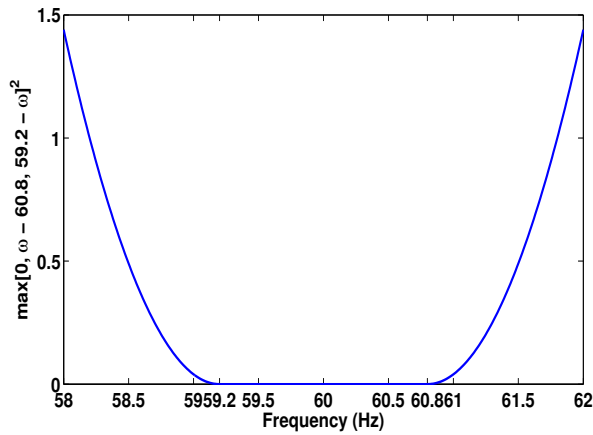


Fig. 2. Dynamics security penalty measure

exceed the set limits. Generator 2 has the most frequency excursion because of its close proximity to the fault location.

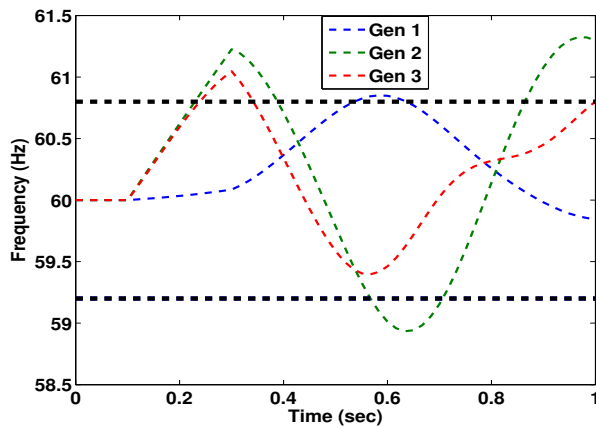


Fig. 3. Generator frequencies from an OPF solution for a 12-cycle 3-phase fault at Bus 7

A similar dynamically insecure behavior is observed for a fault at Bus 9, as seen from Fig. 4. In this case, Gen3 has the most frequency deviation as it is closest to the fault location.

### B. Dynamic security constrained OPF for a fault at Bus 7

The generation schedule for the DSOPF for a fault at Bus 7 is given in Table II. With the frequency limits enforced, the generation is rescheduled with Gen2 reducing its output, while Gen1's output is increased. The frequency of the three generators, as shown in Fig. 5, is constrained within the set frequency limits due to the inclusion of the frequency limits in the OPF. The total cost for this generation schedule, \$6509.62/hr, is higher since the cheapest generator's output is reduced. The Lagrange multipliers for the inequality constraints yields the marginal cost associated for keeping the frequency within the limits. As seen, generators 2 and 3 have a higher marginal cost since they have the most frequency deviation.

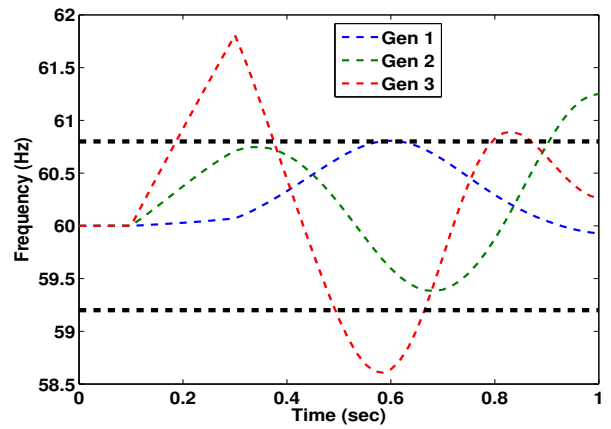


Fig. 4. Generator frequencies from an OPF solution for a 12-cycle 3-phase fault at Bus 9

TABLE II  
GENERATION SCHEDULE WITH DYNAMIC CONSTRAINTS FOR A 12-CYCLE 3-PHASE FAULT AT BUS 7

Generator	Bus Number	MW	Marginal Cost (\$/Hz)
Gen1	1	173.53	100.00
Gen2	2	87.48	773.23
Gen3	3	59.39	621.11

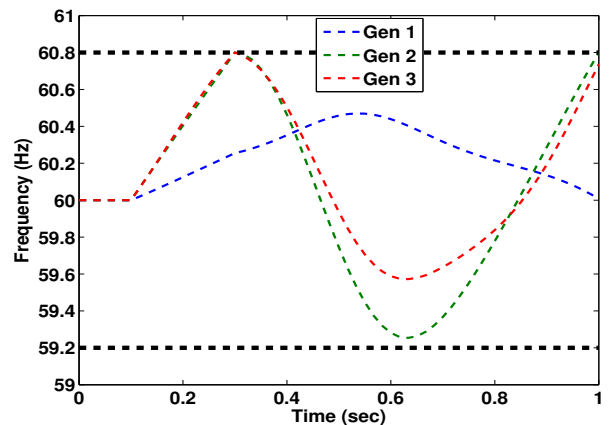


Fig. 5. Generator frequencies from DSOPF solution for a 12-cycle 3-phase fault at Bus 7

### C. Dynamic security constrained OPF for a fault at Bus 9

The generation schedule obtained from DSOP for a fault at Bus 9 is given in Table III. As seen, the generation gets rescheduled such that Gen3's output is reduced significantly and it is provided by Gen1 and Gen2. The total cost for this schedule is \$6201.64/hr.

## VII. SUMMARY

A novel approach for determining dynamic security constrained optimal power flow using finite-differencing sensitivities was discussed in this paper. Results for different fault scenarios for a 9-bus system show the validity of the proposed

TABLE III

GENERATION SCHEDULE WITH DYNAMIC CONSTRAINTS FOR A 12-CYCLE 3-PHASE FAULT AT BUS 9

Generator	Bus Number	MW	Marginal Cost (\$/Hz)
Gen1	1	154.73	20.00
Gen2	2	124.97	660.94
Gen3	3	39.59	445.38

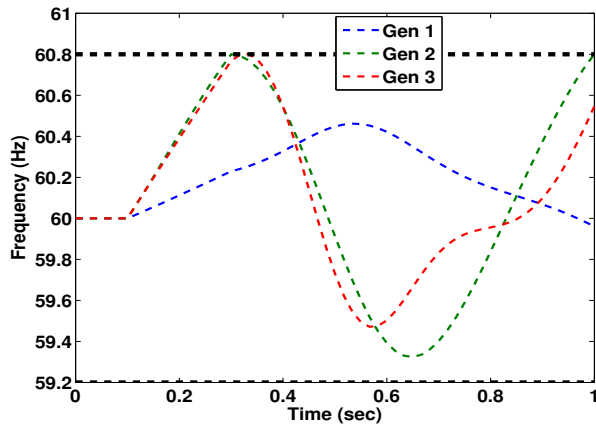


Fig. 6. Generator frequencies from DSOPF solution for a 12-cycle 3-phase fault at Bus 9

formulation. The formulation also provides the marginal cost of generator frequency deviation.

## ACKNOWLEDGMENTS

This work was supported by U.S. Dept. of Energy, Office of Science, Advanced Scientific Computing Research, under Contract DE-AC02-06CH11357.

## REFERENCES

- [1] Northern American Electric Reliability Corporation. Frequency response initiative report: The reliability role of frequency response. Technical report, Northern American Electric Reliability Corporation, 2012.
- [2] A.A. Fouad and T. Jianzhong. Stability constrained optimal rescheduling of generation. *IEEE Transactions on Power Systems*, 8(1):105–112, 1993.
- [3] La Scala M., Trovato M., and Antonelli C. On-line dynamic preventive control: an algorithm for transient security dispatch. *IEEE Transactions on Power Systems*, 13(2):601–610, 1998.
- [4] D. Gan, R.J. Thomas, and R.D. Zimmerman. Stability-constrained optimal power flow. *IEEE Transactions on Power Systems*, 15(2):535–540, 2000.
- [5] Yamashiro S. On-line secure-economy preventive control of power systems by pattern recognition. *IEEE Transactions on Power Systems*, 1(3), 1986.
- [6] Kita H., Hasegawa J., Sato N., and Nishiya K. Dynamic preventive control for power system using transient stability assessment based on pattern recognition. *Electrical Engineering in Japan*, 115(4), 1995.
- [7] Sobajic D. J. and Pao Y. H. Artificial neural-net based security assessment for electric power systems. *IEEE Transactions on Power Systems*, 4(1), 1989.
- [8] Miranda V., Fidalgo J. N., Pecas Lopes J. A., and Almeida L. B. Real-time preventive actions for transient stability enhancement with a hybrid neural network - optimization approach. *IEEE Transactions on Power Systems*, 10(2), 1995.
- [9] Bettiol A. L., Wehenkel L., and Pavella M. Transient stability constrained maximum allowable transfer. *IEEE Transactions on Power Systems*, 14(2), 1999.
- [10] Chen L., Tada Y., Okamoto H., Tanabe R., and Ono A. Optimal operation solutions of power systems with transient stability constraints. *IEEE Transactions on Circuits and Systems*, 48(3), 2001.
- [11] Yue Yuan, J. Kubokawa, and H. Sasaki. A solution of optimal power flow with multicontingency transient stability constraints. *IEEE Transactions on Power Systems*, 18(3):1094–1102, 2003.
- [12] Hguyen T. and Pai M. A. Dynamic security-constrained rescheduling of power systems using trajectory sensitivities. *IEEE Transactions on Power Systems*, 18(2), 2003.
- [13] Sun Y., Xinlin Y., and Wang H. F. Approach for optimal power flow with transient stability constraints. In *IEE Generation, Transmission, and Distribution*, volume 151, pages 8–18, 2004.
- [14] N. Mo, Z. Y. Zou, K.W. Chan, and T. Y G Pong. Transient stability constrained optimal power flow using particle swarm optimisation. *Generation, Transmission Distribution, IET*, 1(3):476–483, 2007.
- [15] Zwe-Lee Gaing and Xun-Han Liu. New constriction particle swarm optimization for security-constrained optimal power flow solution. In *International Conference on Intelligent Systems Applications to Power Systems, 2007.(ISAP 2007)*, pages 1–6, 2007.
- [16] K.Y. Chan, S.H. Ling, K. W. Chan, H.H.-C. Iu, and G. T Y Pong. Solving multi-contingency transient stability constrained optimal power flow problems with an improved GA. In *IEEE Congress on Evolutionary Computation, 2007. (CEC 2007)*, pages 2901–2908, 2007.
- [17] K. Tangpatiphan and A. Yokoyama. Evolutionary programming incorporating neural network for transient stability constrained optimal power flow. In *Joint International Conference on Power System Technology. (POWERCON)*, pages 1–8, 2008.
- [18] H. R. Cai, C.Y. Chung, and K.P. Wong. Application of differential evolution algorithm for transient stability constrained optimal power flow. *IEEE Transactions on Power Systems*, 23(2):719–728, 2008.
- [19] K. Tangpatiphan and A. Yokoyama. Adaptive evolutionary programming with neural network for transient stability constrained optimal power flow. In *15th International Conference on Intelligent System Applications to Power Systems, 2009. (ISAP '09)*, pages 1–6, 2009.
- [20] A. Hoballah and I. Erlich. PSO-ANN approach for transient stability constrained economic power generation. In *IEEE PowerTech, 2009*, pages 1–6, 2009.
- [21] Jun Wang, Xingguo Cai, and Dongdong Wang. Study of dynamic available transfer capability with the improved differential evolution algorithm. In *International Conference on Energy and Environment Technology, 2009. (ICEET '09)*, volume 2, pages 300–304, 2009.
- [22] Quanyuan Jiang and Zhiguang Huang. An enhanced numerical discretization method for transient stability constrained optimal power flow. *IEEE Transactions on Power Systems*, 25(4):1790–1797, 2010.
- [23] Rainer Hettich and Kenneth O Kortanek. Semi-infinite programming: theory, methods, and applications. *SIAM review*, 35(3):380–429, 1993.
- [24] Craig T Lawrence and Andre L Tits. Feasible sequential quadratic programming for finely discretized problems from sip. In *Semi-Infinite Programming*, pages 159–193. Springer, 1998.
- [25] J Nocedal and J. Wright, S. *Numerical Optimization*. Springer, New York, Berlin, Heidelberg, 1999.
- [26] KL Teo and LS Jennings. Nonlinear optimal control problems with continuous state inequality constraints. *Journal of Optimization Theory and Applications*, 63(1):1–22, 1989.
- [27] Kirby J., Dyer J., Martinez C., Shoreshi R. A., Guttromson R., and Dagle J. Frequency control concerns in the north american electric power system. Technical report, Oak Ridge National Laboratory, 2002.
- [28] Y. Xia, K.W. Chan, and M. Liu. Direct nonlinear primal-dual interior-point method for transient stability constrained optimal power flow. *IEE Proceedings on Generation, Transmission and Distribution*, 152(1):11–16, 2005.
- [29] P. Sauer and M. A. Pai. *Power System Dynamics and Stability*. Prentice Hall Inc., 1998.
- [30] Ray Zimmerman and C. Murillo-Sanchez. Matpower 4.0 users manual. Technical report, Power Systems Engineering Research Center, 2011.

Government License: The submitted manuscript has been created by UChicago Argonne, LLC, Operator of Argonne National Laboratory (“Argonne”). Argonne, a U.S. Department of Energy Office of Science laboratory, is operated under Contract No. DE-AC02-06CH11357. The U.S. Government retains for itself, and others acting on its behalf, a paid-up nonexclusive, irrevocable worldwide license in said article to reproduce, prepare derivative works, distribute copies to the public, and perform publicly and display publicly, by or on behalf of the Government.